Geochemistry and U–Pb protolith ages of eclogitic rocks of the Asís Lithodeme, Piaxtla Suite, Acatlán Complex, southern Mexico: tectonothermal activity along the southern margin of the Rheic Ocean

J. BRENDAN MURPHY[1], J. DUNCAN KEPPIE[2], R. DAMIAN NANCE[3], BRENT V. MILLER[4], JAROSLAV DOSTAL[5], MATT MIDDLETON[1], JAVIER FERNANDEZ-SUÁREZ[6] TERESA E. JEFFRIES[7] & CRAIG D. STOREY[8]

[1]*Department of Earth Sciences, St. F. X. University, Antigonish, NS, Canada, B2G 2W5 (e-mail: bmurphy@stfx.ca)*

[2]*Instituto de Geología, Universidad Nacional Autónoma de México, 04510 México D.F., Mexico*

[3]*Department of Geological Sciences, Ohio University, Athens, OH 45701, USA*

[4]*Department of Geology and Geophysics, Texas A&M, College Station, TX 77843-3115, USA*

[5]*Department of Geology, St. Mary's University, Halifax, NS, Canada B2H 3C3*

[6]*Departamento de Petrología y Geoquímica, Universidad Complutense, 28040 Madrid, Spain*

[7]*Natural History Museum, Cromwell Road, London SW7 5BD, UK*

[8]*Department of Earth Sciences, Open University, Walton Hall, Milton Keynes MK7 6AA, UK*

Abstract: Recent data indicating that the Piaxtla Suite (Acatlán Complex, southern Mexico) underwent eclogite-facies metamorphism and exhumation during the Devono-Carboniferous suggest an origin within the Rheic Ocean rather than the Iapetus Ocean. The Asís Lithodeme (Piaxtla Suite) consists of polydeformed metasediments and eclogitic amphibolites that are intruded by megacrystic granitoid rocks. U–Pb (zircon) data indicate that the metasediments were deposited after *c*. 700 Ma and before intrusion of *c*. 470–420 Ma quartz-augen granite. The metasedimentary rocks contain abundant Mesoproterozoic detrital zircons (*c*. 1050–1250 Ma) and a few zircons in the range of *c*. 900–992 and *c*. 1330–1662 Ma. Their geochemical and Sm–Nd isotopic signature is typical of rift-related, passive margin sediments derived from an ancient cratonic source, which is interpreted to be the adjacent Mesoproterozoic Oaxacan Complex. Megacrystic granites were derived by partial melting of a *c*. 1 Ga crustal source, similar to the Oaxacan Complex. Amphibolitic layers exhibit a continental tholeiitic geochemistry, with a *c*. 0.8–1.1 Ga source (T_{DM} age), and are inferred to have originated in a rift-related environment by melting of lithospheric mantle in the Ordovician. This rifting may be related to the Early Ordovician drift of peri-Gondwanan terranes (e.g. Avalonia) from Gondwana and the origin of the Rheic Ocean.

The Acatlán Complex of southern Mexico (Fig. 1) contains eclogitic metasedimentary and metaigneous rocks (Piaxtla Suite) that have been inferred to be vestiges of the Cambro-Ordovician Iapetus oceanic lithosphere (Ortega-Gutiérrez *et al*. 1999; Meza-Figueroa *et al*. 2003). This proposition was based on the interpretation that most of these rocks represent an ophiolitic complex that was subducted beneath Laurentia and underwent exhumation and dehydration to produce megacrystic granites (Esperanza granitoids dated at 440 ± 14 Ma: lower intercept U–Pb zircon age, Ortega-Gutiérrez *et al*. 1999: more recently dated at 471 ± 13 Ma: concordant U–Pb laser ablation inductively coupled plasma mass spectrometry (LA-ICP-MS) zircon age, Sánchez-Zavala *et al*. 2004). Alternatively, Keppie & Ramos (1999) and Keppie (2004) suggested that the Acatlán Complex formed on the southern margin of the Ordovician–Carboniferous Rheic Ocean and did not collide with Laurentia until the Carboniferous during the amalgamation of Pangaea. To resolve this problem, which is fundamental to the Palaeozoic evolution of the Iapetus and Rheic oceans and to continental reconstructions, we have commenced a detailed field study of these eclogitic rocks combined with geochemistry and precise geochronology. In a companion paper, Middleton *et al*. (2005) have outlined the Carboniferous subduction and exhumation history of one of these eclogite-bearing units, the Asís Lithodeme; this is consistent with destruction of the Rheic Ocean but not with the Iapetus Ocean, which was closed by the Silurian. This paper presents geochemical and geochronological data for the Asís Lithodeme of the Piaxtla Suite, and focuses on the tectonic setting of the protoliths (Fig. 1). These data document a protolith association of continental tholeiites, continentally derived sediments and *c*. 470–420 Ma megacrystic granitoids inferred to form part of a rift–passive margin sequence, and that developed along the southern flank of the Rheic Ocean (northern margin of Gondwana: present coordinates) in Mexico (Oaxaquia terrane: Keppie 2004).

Geological setting

The Acatlán Complex of the Mixteca terrane in southern Mexico is juxtaposed on its eastern side against the *c*. 1 Ga Oaxaquia terrane, and the terrane boundary is a Permian dextral flower structure (Fig. 1) (Elías-Herrera & Ortega-Gutiérrez 2002). Until recently, the Acatlán Complex was inferred to have undergone the following sequence of events (Fig. 2, left-hand side): (1) Cambro-Ordovician deposition of the clastic Petlalcingo Group (Magdalena, Chazumba and Cosoltepec formations) and oceanic Piaxtla Group (Xayacatlán Formation and Esperanza granitoids); (2) Late Ordovician–Early Silurian polyphase

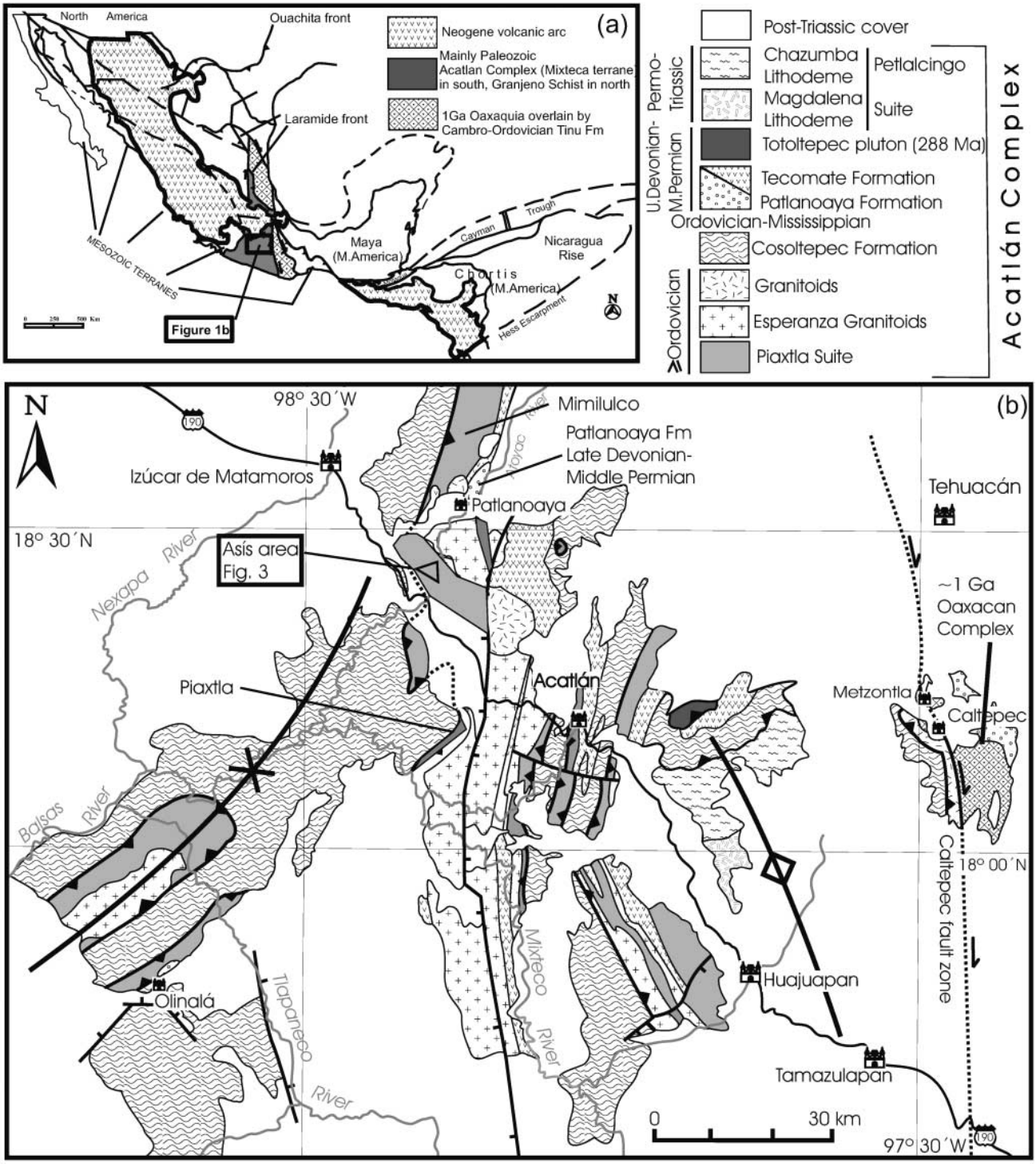

Fig. 1. (**a**) Terrane map of Mexico showing the location of the Acatlán Complex (after Keppie 2004); (**b**) geological map of the Acatlán Complex (modified after Keppie *et al*. 2005) showing the location of the Asís area.

deformation during the Acatecan Orogeny, when the Piaxtla Group underwent eclogite-facies metamorphism and was thrust over the Petlalcingo Group metamorphosed at greenschist facies; (3) Devonian deposition of the Tecomate Formation; (4) Devonian deformation and greenschist-facies metamorphism during the Mixtecan Orogeny; (5) deposition of latest Devonian–Mid-Permian sedimentary rocks of the Otates and Patlanoaya formations (Ortega-Gutiérrez *et al*. 1999; Sánchez Zavala *et al*. 2000). Meza-Figueroa *et al*. (2003) have suggested that eclogitic rocks of the Piaxtla Suite at Piaxtla and Mimilulco lying on either side of the Asís area (Fig. 1b) represent mid-ocean ridge basalt (MORB), ocean island basalt (OIB) and island arc basaltic rocks that were metamorphosed to 11–15 kbar and 560 ± 60 °C (Fig. 1), conditions typical of low- to

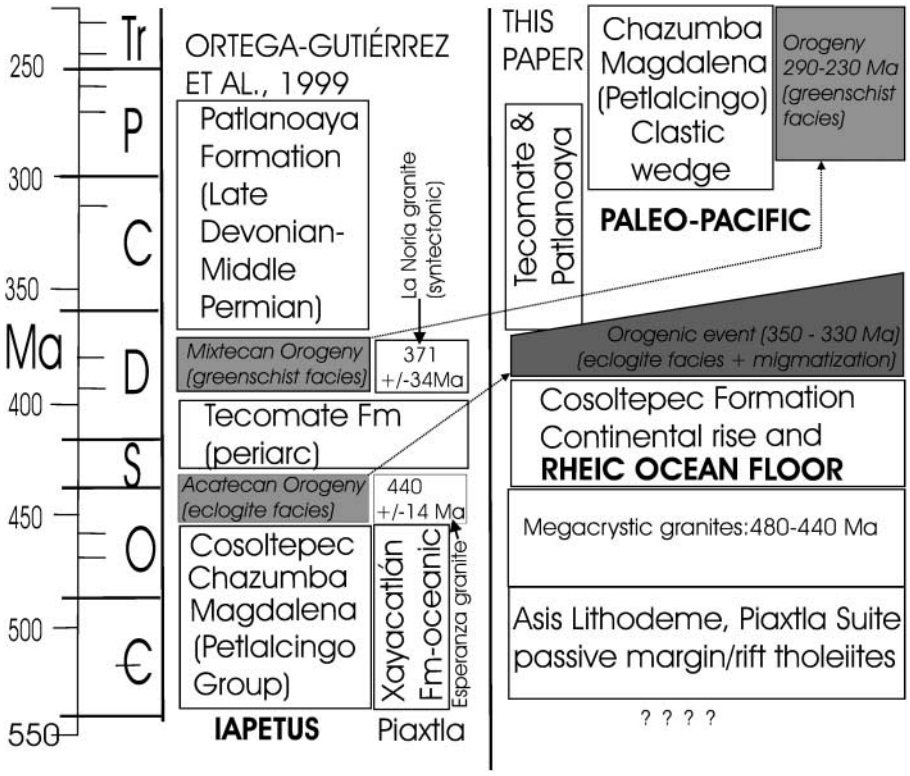

Fig. 2. Time and space diagram showing the tectonostratigraphy of the Acatlán Complex after Ortega-Gutiérrez *et al*. (1999) and this paper. The Cosoltepec upper boundary allows for deposition after 410 Ma to accommodate recent data of Talavera-Mendoza *et al*. (2005).

medium-temperature eclogites developed in alpine-type tectonic settings (Carswell 1990).

However, recent work has shown the following (Fig. 2, right-hand side): (1) the Magdalena and Chazumba units are Permo-Triassic, whereas part of the Cosoltepec Formation is bracketed between rocks of *c*. 455 Ma age and the base of unconformably overlying uppermost Devonian sedimentary rocks (Vachard & Flores de Dios 2002; Derycke-Khatir *et al*. 2005; Keppie *et al*. 2006), whereas other parts of the Cosoltepec Formation are younger than *c*. 410 Ma (post-Silurian: Talavera-Mendoza *et al*. 2005); (2) the Tecomate Formation is of latest Carboniferous–Mid-Permian age (Keppie *et al*. 2004*a*); (3) the type-Xayacatlán igneous body is of earliest Silurian age and has a continental tholeiitic signature (Dostal *et al*. 2004): other units previously correlated with the Xayacatlan Formation are bracketed between *c*. 870 Ma and *c*. 470 Ma (Talavera-Mendoza *et al*. 2005); (4) the tectonothermal events are Devono-Mississippian (eclogite-facies metamorphism: Middleton *et al*. 2005), Permo-Triassic (greenschist-facies metamorphism: Malone *et al*. 2002; Keppie *et al*. 2004*a*, 2006), and Jurassic (local migmatization and high-temperature–low-pressure metamorphism: Keppie *et al*. 2004*b*); although Talavera-Mendoza *et al*. (2005) interpreted Ordovician granitoid ages in terms of Taconian–Salinian orogenic events, we suggest that they represent intrusive ages. This has led to reclassifying the Magdalena and Chazumba units as lithodemes of a restricted Petlalcingo Suite (Keppie *et al*. 2006). Similarly, the Piaxtla Group is replaced by the Piaxtla Suite containing the Asís Lithodeme, but excluding the megacrystic granitoids: the significant age difference between the Asís Lithodeme and the Xayacatlán unit suggests they should not be correlated.

Lithologies and field relations

The Asís Lithodeme of the Piaxtla Suite is composed mainly of metapsammitic and metapelitic rocks, and amphibolites, many of which are migmatized, which are intruded by megacrystic granites, the margins of which are mylonitized (Fig. 3). As all contacts are tectonic, the original relationships between the various rock types are uncertain. However, as the amphibolites

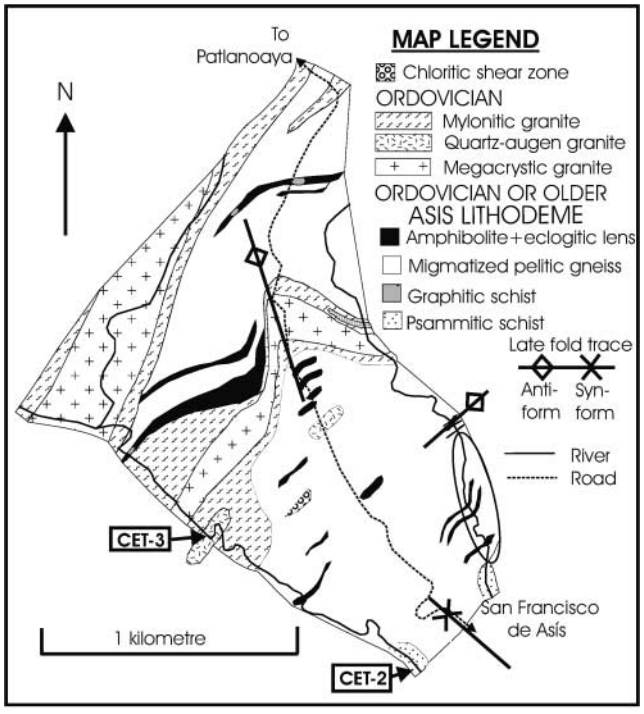

Fig. 3. Geological map of the San Francisco de Asís area (18°27.6–29.4′N, 98°17.7–19.1′W).

are always thin bands and lenses, they may have been either minor intrusive rocks or lavas within the metasedimentary rocks. The presence of xenoliths of the metasedimentary rocks within associated megacrystic granitoids could reflect an original intrusive relationship, but this remains to be confirmed. The occurrence of the quartz-augen granite within the K-feldspar megacrystic granite also suggests an original intrusive relationship that may, or may not, have been part of the same magmatic episode. The *P–T* paths of the different lithologies indicate that they share a similar retrograde path (Middleton *et al*. 2005).

The pelitic metasedimentary rocks consist mainly of quartz, plagioclase, biotite and phengite, minor garnet and rutile, and secondary chlorite, calcite and hematite. The metapsammitic rocks are composed mainly of quartz with minor plagioclase, biotite and muscovite, and accessory opaque minerals. Migmatization of these metasedimentary rocks is preferentially developed in the pelitic metasedimentary rocks.

The amphibolites are composed mainly of albite and aligned amphibole with rare omphacite inclusions, minor epidote, phengite, biotite, garnet, and quartz, and accessory hematite, chlorite, titanite, ilmenite, fluorite, and calcite. Migmatitic leucosomes are present in many of the amphibolites.

The megacrystic granitoids are composed of quartz and albite, with minor phengite and secondary chlorite. Megacrysts are generally K-feldspar or quartz, with minor garnet. Quartz-augen granite occurs as small bodies within the K-feldspar granite and within the migmatitic metasedimentary rocks (Fig. 3). A few aplitic sheets cut the granitoids and have essentially the same mineralogy with the addition of secondary epidote.

Geochronology

Analytical methods

Two representative samples were collected for U–Pb isotopic analysis. A psammitic gneiss (CET-2: UTM 74.675, 38.902) was analysed using LA-ICP-MS at the Natural History Museum, London, and a quartz-augen granite from the megacrystic granite unit (CET-3: UTM 73.489, 39.515) was analysed by sensitive high-resolution ion microprobe (SHRIMP) at Stanford University (Fig. 3). The psammitic gneiss is composed mainly of quartz, plagioclase, biotite and muscovite, with accessory garnet and opaque minerals. The quartz-augen granite is composed of quartz and plagioclase (albite), with minor muscovite (phengite) and secondary chlorite. Analytical methods and LA-ICP-MS U–Pb analyses are available online at http://www.geolsoc.org.uk/SUP18237. A hard copy can be obtained from the Society Library.

Zircons were separated from psammitic sample CET-2 at the Complutense University of Madrid following conventional techniques. Details of the separation procedure have been given by Fernández-Suárez *et al*. (2002) and Jeffries *et al*. (2003) Analytical instrumentation, analytical protocol and methodology, data reduction, age calculation and common Pb correction followed those described by Fernández-Suárez *et al*. (2002), Jeffries *et al*. (2003) and Murphy *et al*. (2004).

Selected zircon grains from the quartz-augen granite sample (CET-3) were mounted in epoxy, polished, imaged in cathodoluminescence and photographed under reflected light, then gold-coated prior to analysis. Uranium–lead isotopes were analysed by SHRIMP-RG (SHRIMP-reverse geometry) at Stanford University following techniques described by Degraaff-Surpless *et al*. (2002). Errors in Table 1 are quoted at 1σ and ellipses on concordia diagrams are shown at the 68.3% confidence level.

Results

Seventy-two analyses, all representing one analysis per grain, were performed on zircons from psammitic sample CET-2. Of those, seven were rejected based on the presence of features such as discordance >10%, high common Pb detected in the U–Pb, Th–Pb, Pb–Pb isotope ratio plots, and/or elemental U–Pb fractionation or inconsistent behavior of U–Pb and Th–Pb ratios in the course of ablation (see Jeffries *et al*. 2003). Figure 4 shows concordia plots and a combined binned frequency and probability density distribution plot for the sample. Where the analyses overlap concordia with MSWD of concordance <2, we assign a U–Pb concordia age (see Ludwig 1998) as the best age estimate. Where analyses are normally discordant (i.e. they plot below concordia), we assign the $^{207}Pb/^{206}Pb$ age and error, as we are confident that any discordance is not a result of excess common Pb in the analysis or analytically induced problems such as laser-induced elemental fractionation (for details see Jeffries *et al*. 2003). Consequently, these ages will approximate the 'correct' age, assuming a zero-age Pb-loss event, and there is a small danger that a non-zero-age thermal event could result in these ages representing minimum ages. However, the amount of discordance within these zircons is minor (Fig. 4) and therefore this phenomenon is unlikely to affect any of the main conclusions reached regarding this dataset.

As shown in Figure 4 most analyses of psammitic sample CET-2 yielded Mesoproterozoic ages with a predominance of zircons in the age range *c*. 1050–1250 Ma (*c*. 75% of analyses). Five zircons yielded older Mesoproterozoic ages at *c*. 1330, 1332, 1486, 1540 and 1560 Ma, and one zircon yielded a late Palaeoproterozoic age of *c*. 1662 Ma. Nine zircons yielded early Neoproterozoic (Tonian) ages between *c*. 900 and 992 Ma. Finally, only one grain (Fig. 4c) yielded a younger Neoproterozoic (Cryogenian) age of 705 ± 8 Ma, the youngest grain dated in the sample.

The SHRIMP analyses of zircons from the quartz-augen granite (CET-3) yielded concordant ages ranging from 470 to

Table 1. *U–Pb isotopic data for quartz-augen granite (SHRIMP; sample CET-3; UTM 73.489, 39.515), Asís Lithodeme*

Sample and spot no.	U (ppm)	Th (ppm)	$^{206}Pb^*$ (ppm)	Atomic ratios						Ages (Ma)		ρ‡
				$^{206}Pb/^{238}U$	% Error†	$^{207}Pb/^{235}U$	% Error†	$^{207}Pb/^{206}Pb$	% Error†	$^{206}Pb/^{238}U$	$^{207}Pb/^{206}Pb$	
CET3-1	292	185.2	17.5	0.06949	0.870	0.48700	4.800	0.05090	4.700	433	234	0.18
CET3-2	406	205.4	26.1	0.07470	0.500	0.59700	1.500	0.05796	1.400	464	528	0.33
CET3-3	295	137.4	17.4	0.06821	0.600	0.51100	4.900	0.05440	4.900	425	386	0.12
CET3-4	468	353.0	30.3	0.07520	0.450	0.59130	1.400	0.05702	1.300	467	492	0.33
CET3-5	319	137.5	20.2	0.07353	0.550	0.56400	2.300	0.05570	2.200	457	439	0.24
CET3-6	2166	671.0	199.0	0.10602	0.290	1.02500	2.000	0.07010	2.000	650	931	0.15

Pb* indicates radiogenic Pb concentrations.
†Errors are 1σ. Error in standard calibration was 0.34–0.55% (not included in above errors but required when comparing data from different sources).
‡$^{207}Pb/^{235}U$–$^{206}Pb/^{238}U$ correlation coefficient of Ludwig (1989).

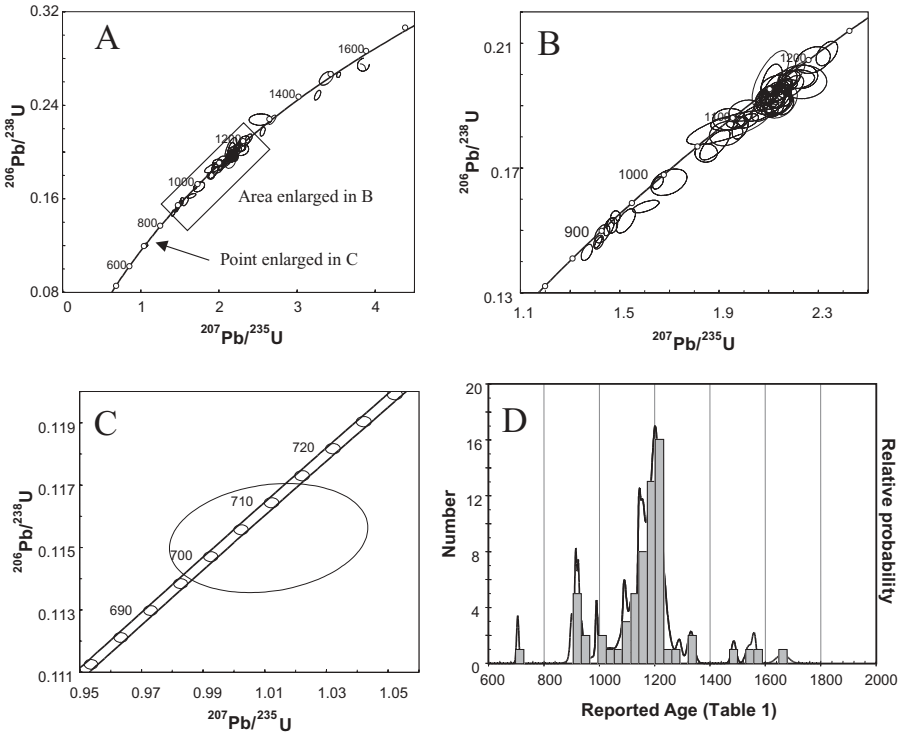

Fig. 4. (**a**) Concordia plot of U–Pb zircon analyses of psammitic sample CET-2; ellipses represent 2σ uncertainties. (**b**) Enlargement of (**a**) showing a detail of the two main Mesoproterozoic populations at *c*. 1050–1250 and 900–990 Ma. (**c**) Detail of the youngest grain dated in sample CET-2. (d) Combined binned frequency and probability density distribution plot, with the data (available online see p. 686) shown as 'reported age'.

420 Ma and two discordant analyses with $^{207}Pb/^{206}Pb$ ages ranging from *c*. 234 Ma to *c*. 931 Ma (Fig. 5, Table 1).

Interpretation

The youngest *c*. 705 Ma detrital zircon from the metapsammite (CET-2) provides an older limit for the time of deposition. A younger limit of *c*. 470–420 Ma is provided by the presence of metasedimentary xenoliths in the quartz-augen granite, assuming that the xenoliths were derived from the country rocks.

Beyond broadly constraining the intrusive age of the megacrystic granite, the 470–420 Ma spread in the ages of the quartz-augen granite sample CET-3 is problematic. Although lithologically and geochemically similar to other *c*. 470 Ma megacrystic granitoid rocks in the Mixteca terrane (e.g. Keppie 2004), determining whether the Asís quartz-augen granite is correlative with other Ordovician–Silurian granitoid bodies in the Mixteca terrane will take more detailed analysis.

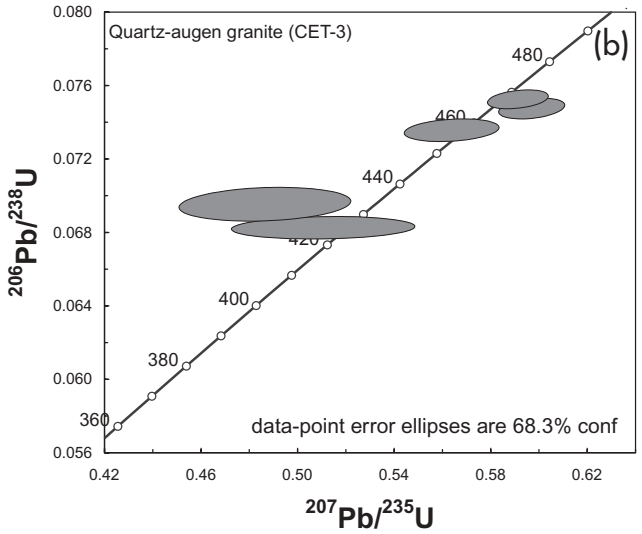

Fig. 5. SHRIMP data for zircon from the quartz-augen granite, sample CET-3, plotted on a concordia diagram.

Geochemistry

Analytical methods

Twenty samples of amphibolite, four samples of pelitic and psammitic gneiss, 18 samples of granite (seven megacrystic, 11 mylonitic), and 27 samples of migmatite were collected for chemical analyses. The samples were analysed by X-ray fluorescence spectrometry for major and several trace elements (Rb, Sr, Ba, Zr, Nb, Y, Zn, V, Cr and Ni) in the Nova Scotia Regional Geochemical Centre at Saint Mary's University, Halifax. From this set, 24 samples (five amphibolite, two pelitic–psammitic gneiss, seven granite, 10 migmatite) were selected for additional trace elements analyses (rare earth elements (REE), Hf, Zr, Nb, Ta and Th) by ICP-MS in the Geochemical Laboratory of the Ontario Geological Survey in Sudbury, Ontario, and for Sm–Nd isotopic analyses, which were performed at Memorial University, Newfoundland. All geochemical and isotopic data are available online in supplementary files (see p. 686).

Precision and accuracy of the X-ray data have been reported by Dostal *et al*. (1986) and for ICP-MS data by Ayer & Davis (1997). Briefly, analytical errors for trace elements are generally <5 rel. %. Analytical procedures for the Sm–Nd isotopic analyses have been described by Kerr *et al*. (1995). To facilitate comparison between the various lithological units, $\epsilon_{Nd(t)}$ values quoted in the text are for $t = 475$Ma.

The use of chemical data of rocks metamorphosed under high-grade conditions for tectonic models assumes that the elements under consideration remained essentially immobile during secondary processes. There are several lines of evidence to suggest that most major elements, such as Si, Al, Mg, Fe and Ti, as well as many trace elements including high field strength elements (HFSE; Zr, Hf, Nb, Y, Ta, and Th), REE and

the transition elements (Cr, Ni and V) were not redistributed in the analysed rocks. In particular, their consistent trends and similarities to modern volcanic and sedimentary rocks suggest that they essentially retained the original characteristics.

Results

Amphibolites. With the exception of one sample (101-4, which shows evidence of significant crustal contamination), the amphibolites display remarkably uniform geochemistry and trends consistent with igneous processes. They have characteristics of differentiated tholeiitic basalts, with SiO_2 between about 48 wt% and 52 wt%, FeO_t/MgO ranging from 1.5 to 3.5, high content of FeO_t (11.1–17.1 wt%), and strong correlations between FeO_t/MgO, TiO_2, P_2O_5, V and Zr, indicating enrichment in these elements during fractionation (e.g. Figs 6–8) and Nb/Y between 0.2 and 0.75. The REE patterns (Fig. 9a) show a slight enrichment in light REE (LREE) with $(La/Yb)_n$ ranging between 1.5 and 2.1, and $(La/Sm)_n$ between 1.2 and 1.6 (sample 101-4 has higher LREE enrichment; $La/Yb_n = 8.7$, $La/Sm_n = 3.5$). The shape of trace element patterns is more similar to enriched (E-) than normal (N-) MORB (Fig. 10a and b): N-MORB-normalized patterns are enriched in strongly incompatible elements, such as Th and LREE relative to heavy REE (HREE), whereas E-MORB-normalized patterns are relatively flat. These overall trends are typical of differentiated tholeiitic basalts derived from an E-MORB source. In comparison with calc-alkaline and island arc mafic rocks, the amphibolites have wide ranges in Cr (34–328 ppm) and Ni (35–172 ppm), and also high Ti/V (35–45) and Ti/Zr (60–120), as well as relatively constant Zr/Y (4.0– 6) values, with the exception of two samples with high Zr that have Zr/Y of 8.8 and 10.5. According to Pearce & Norry (1979), mafic rocks with Zr/Y >4 are typical of within-plate basalts (e.g. Fig. 11).

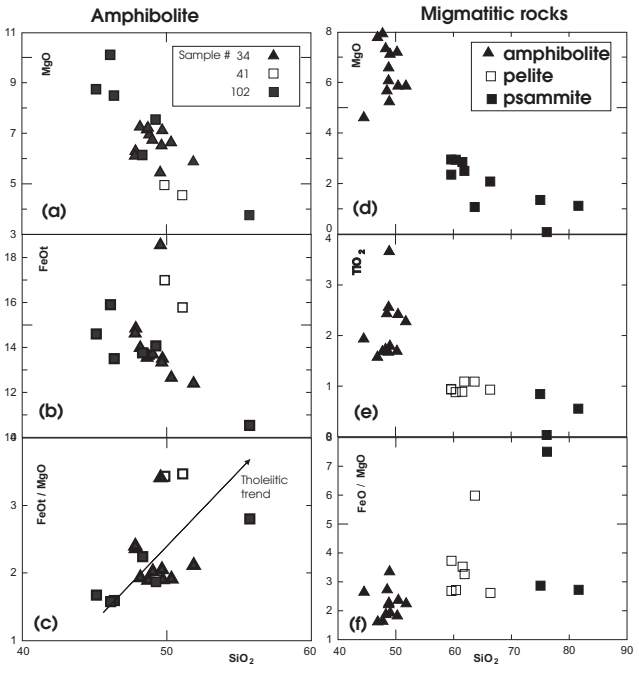

Fig. 6. SiO_2 v. MgO, FeO_t and FeO_t/MgO for the amphibolites (**a**–**c**), and SiO_2 v. MgO, TiO_2 and FeO_t/MgO for the migmatitic rocks (**d**–**f**) of the Asís Lithodeme.

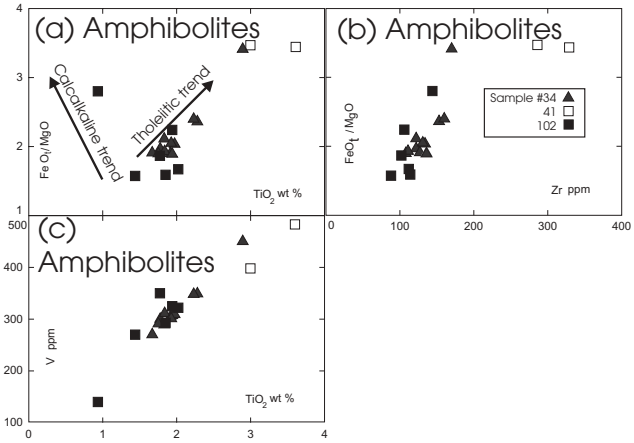

Fig. 7. (**a**) FeO_t/MgO v. TiO_2 (wt%), (**b**) FeO_t/MgO v. Zr and (**c**) V v. TiO_2 for amphibolites of the Asís Lithodeme The lines showing calc-alkaline and tholeiitic trends are after Miyashiro (1974).

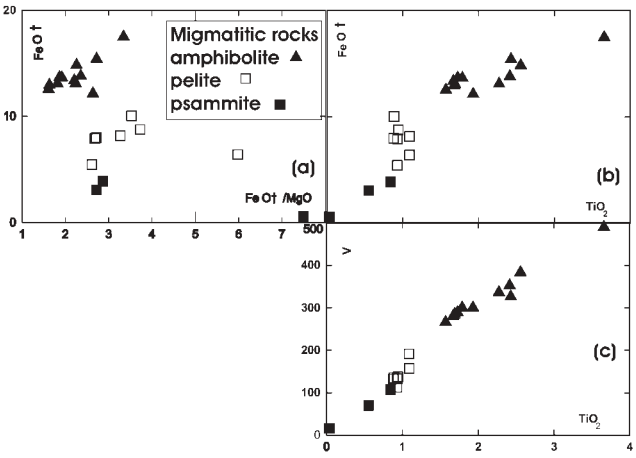

Fig. 8. (**a**) FeO_t v. FeO_t/MgO, (**b**) FeO_t/MgO v. TiO_2 and (**c**) V v. TiO_2 for migmatitic rocks of the Asís Lithodeme.

The Sm–Nd isotopic signature of three of four amphibolite samples is very similar, with $\epsilon_{Nd(t)}$ ranging from +2.8 to +4.6 ($t = 475$Ma), $^{147}Sm/^{144}Nd$ from 0.16 to 0.18 and T_{DM} from 1.09 to 1.27 Ga (Fig. 12a). These $\epsilon_{Nd(t)}$ values are considerably lower than values expected for juvenile magmas from a depleted mantle source. The lack of a discernible negative Nb anomaly on the spidergram plots and low ratios, such as La/Nb (0.7–0.9) and Th/Ta (1.5–2.1), indicate that these low values are not due to crustal contamination and they are interpreted to reflect the original signature of the magma. The contamination of sample 101-4 is clearly indicated by its very low $\epsilon_{Nd(t)}$ of −8.3, low $^{147}Sm/^{144}Nd$ (0.12), high T_{DM} (1.68 Ga), and high La/Nb (2.3).

The migmatized amphibolites are very similar to the amphibolites, having SiO_2 <55%, high contents of FeO_t (12.1–17.4 wt%) high FeO_t/MgO (1.6–2.8), strong correlations between FeO_t, TiO_2, P_2O_5, V and Zr (Fig. 8), and Nb/Y between 0.3 and 0.9, characteristics typical of differentiated tholeiites. Compared with the amphibolites, these mafic migmatites have similar wide ranges in Cr (82–311 ppm) and Ni (45–98 ppm), high Ti/V (35–

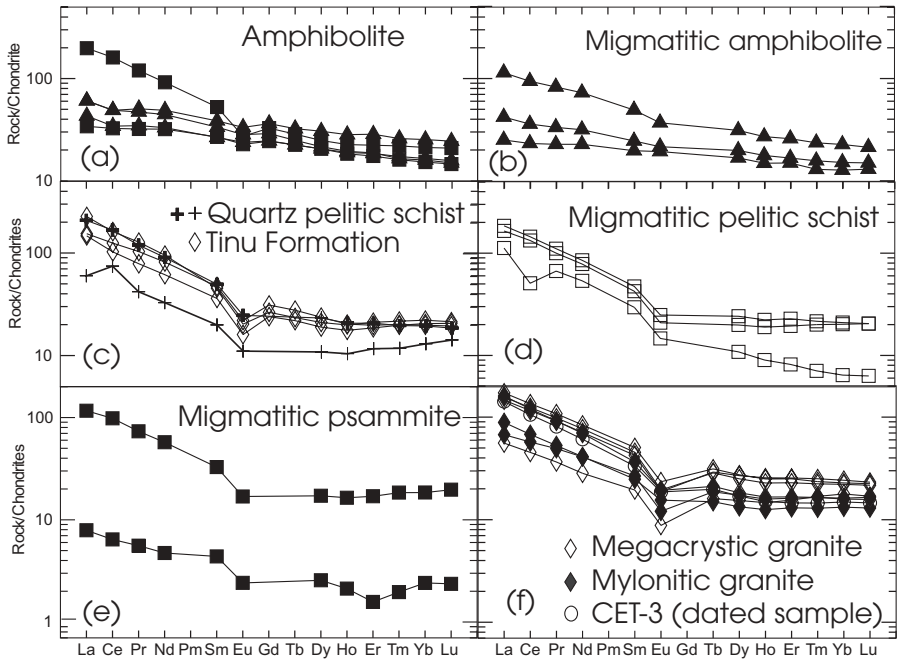

Fig. 9. Spidergrams showing chondrite-normalized REE compositions of rocks from the Asís Lithodeme: (**a**) amphibolite; (**b**) migmatitic amphibolite; (**c**) quartz pelitic schist (data for the Tiñu Formation are from Murphy *et al*. 2005); (**d**) migmatitic pelitic schist; (**e**) migmatitic psammite; (**f**) granitoid rocks.

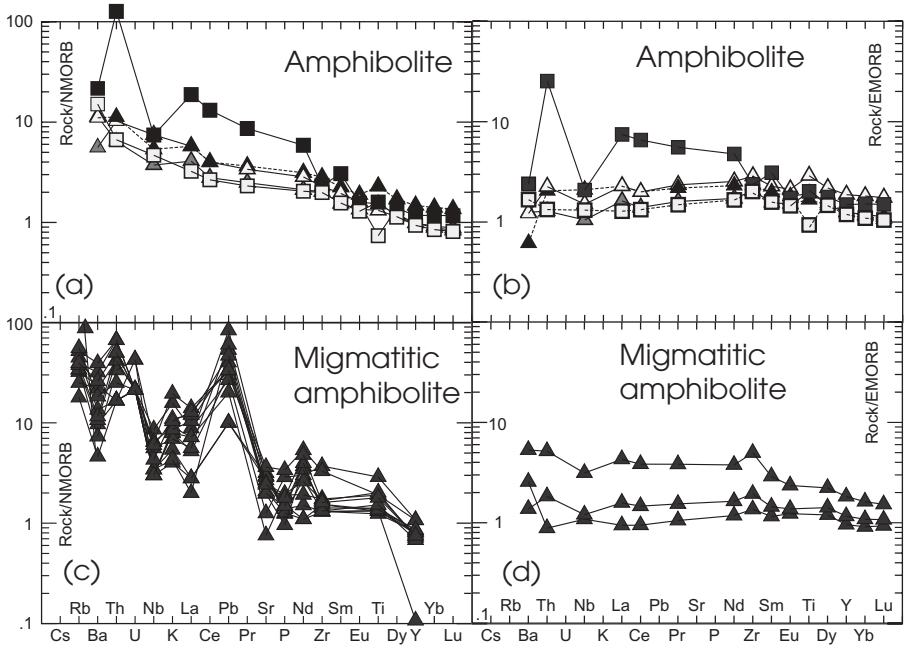

Fig. 10. Spidergrams showing N-MORB- and E-MORB-normalized patterns for amphibolites (**a**, **b**) and migmatic amphibolites (**c**, **d**) from the Asís Lithodeme (normalizing values after Sun & McDonough 1989).

50) and Ti/Zr (80–120) as well as relatively high Zr/Y (4.0–10). The REE patterns also show (Fig. 9b) a slight enrichment in LREE, with $(La/Yb)_n$ ranging between 1.8 and 4.7 and $(La/Sm)_n$ between 1.2 and 2.1, and, as for the amphibolites, the shape of trace element patterns is more similar to E-type than N-type MORB (Fig. 10c and d). The Sm–Nd isotopic signature is also very similar, with $\epsilon_{Nd(t)}$ ranging from +2.0 to +5.8 ($t = 475$Ma), $^{147}Sm/^{144}Nd$ from 0.15 to 0.18 and T_{DM} from 0.75 to 1.25 Ga (Fig. 12). The lack of a discernible negative Nb anomaly on the spidergram plots and low ratios such as La/Nb (0.7–0.75) indicate that crustal contamination was insignificant, and so, as for the amphibolites, these values are interpreted to reflect an original signature that is typical of differentiated tholeiitic basalts derived from an enriched MORB source.

Pelitic and psammitic gneiss. The pelitic and psammitic gneiss is highly variable in chemistry, with SiO_2 ranging from 59.1 to 92.0 wt%. Two samples were analysed for REE and Sm–Nd isotopes, one with low SiO_2 (59 wt%) and one with high SiO_2 (86.5 wt%). These samples show similar chondrite-normalized patterns, with moderately enriched LREE (La/Sm_n 3.1–4.1), and flat HREE (Dy/Yb_n 0.8–1.2), although the more siliceous sample

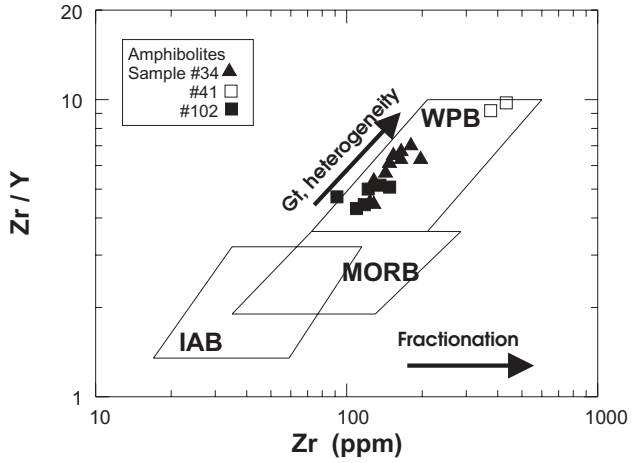

Fig. 11. Zr/Y v. Zr discrimination diagram (after Pearce & Norry 1979) for the Asís Lithodeme amphibolites. IAB, island arc basalt; MORB, mid-ocean ridge basalt; WPB, within-plate basalt.

has lower total REE and low La relative to Ce (Fig. 9c). Similar patterns are also exhibited on a MORB-normalized plot, with the exception of a strong positive Zr anomaly occurring in the more siliceous sample (Fig. 13a). Despite variations in geochemistry, the Sm–Nd isotopic signature of the two samples is very similar, with $\epsilon_{Nd(t)}$ ranging from −7.2 to −7.5 to ($t = 475$Ma), $^{147}Sm/^{144}Nd$ from 0.12 to 0.13, and T_{DM} from 1.68 to 1.86 Ga (Fig. 12).

The migmatized metasedimentary rocks have very similar characteristics to the pelitic and psammitic gneisses (Fig. 6d-f) with SiO_2 contents varying from 55 to 70 wt% SiO_2. The REE patterns are enriched in LREE $(La/Sm)_n$ 3.8 to 4.0 with relatively flat HREE with $(La/Yb)_n$ 1.9 to 8.1 (Figs 9d and e) and strong negative Eu anomalies. MORB-normalized trace element profiles are enriched in strongly incompatible trace elements, including Th and Ba, and LREE, relative to the HREE and HFSE. They display distinct negative anomalies for Nb and Ti (Fig. 13b and c), and have La/Nb values (1.1 to 1.8) typical of crustal input. $\epsilon_{Nd(t)}$ values are more depleted than the granitoid rocks, ranging from −5.9 to −8.5 ($t = 475$Ma), with $^{147}Sm/^{144}Nd$ from 0.11 to 0.12 and T_{DM} from 1.45 to 1.73 Ga. These are values that are typical of Mesoproterozoic continental crust. These $\epsilon_{Nd(t)}$ values are considerably lower than those of the amphibolites, the mafic component of the migmatitic amphibolites and the granitoid rocks, and are typical of an intra-crustal origin.

Although volumetrically minor, migmatites with SiO_2 content >70 wt% can be distinguished from less siliceous migmatites and from granitoid rocks by lower Fe_2O_3, MgO, CaO, TiO_2, Ni, V and Cr and by highly variable REE and HFSE abundances that are either similar to or lower than the 55–70 wt% pelitic

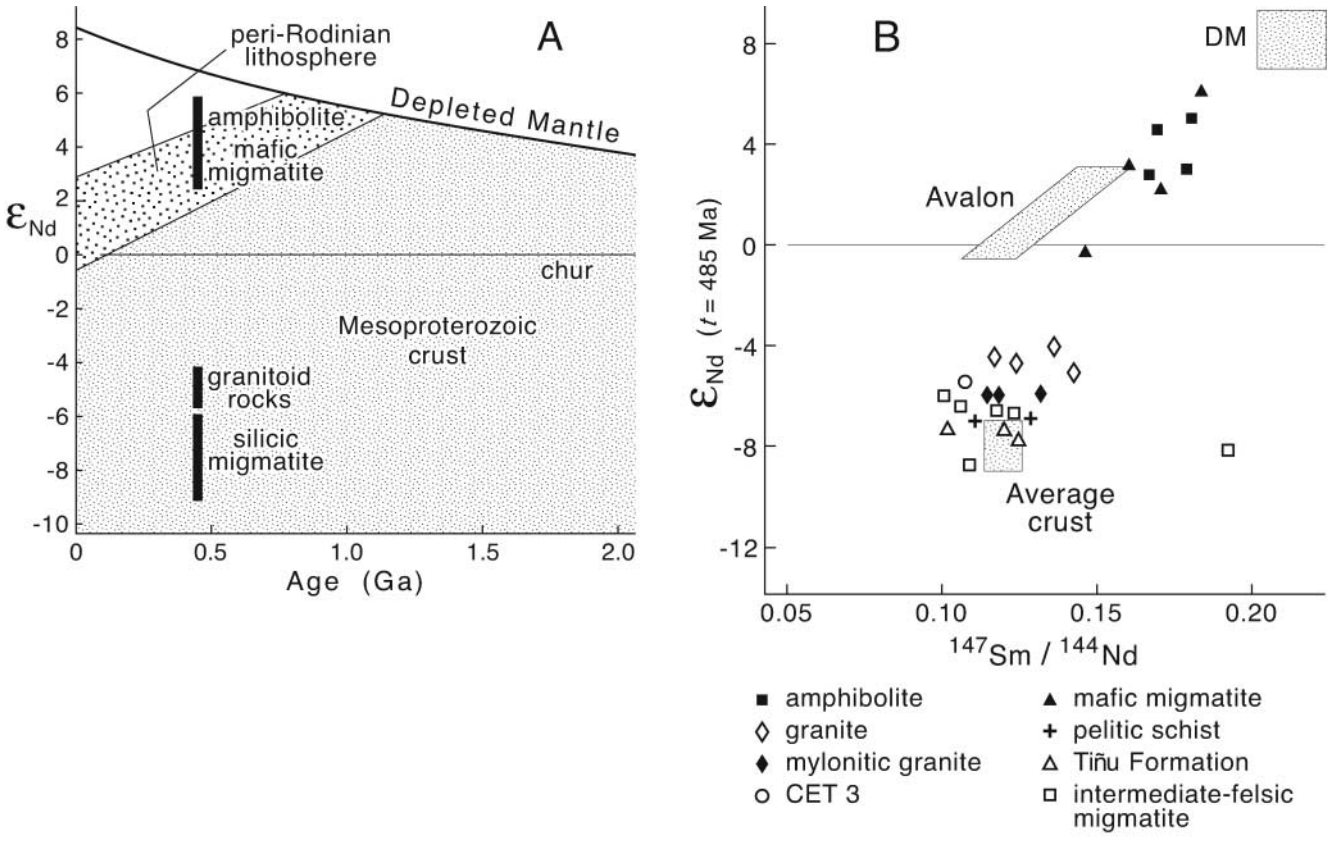

Fig. 12. Sm–Nd isotopic data for the Asís Lithodeme: Asís amphibolites, granitoid rocks and pelitic and psammitic gneisses; and the migmatitic rocks with typical Sm–Nd isotopic compositions of peri-Rodinian oceanic lithosphere (Murphy *et al*. 2000, 2004) and Mesoproterozoic continental crust (after Dickin & McNutt 1989, 1990; Patchett & Ruiz 1987; Daly & McLelland 1991; McLelland *et al*. 1993; Dickin 2000). (**a**) $\epsilon_{Nd(t)}$ v. time comparing Sm–Nd isotopic data; (**b**) $\epsilon_{Nd(t)}$ v. $^{147}Sm/^{144}Nd$ ($t = 475$Ma), comparing the Sm–Nd isotopic data with typical Sm–Nd isotopic compositions of Avalonian crust (Murphy & Macdonald 1993; Murphy *et al*. 1996) and the average upper crust, which is bracketed between modern global average river sediment ($^{147}Sm/^{144}Nd = 0.114$; $T_{DM} = 1.52$Ga; Goldstein & Jacobsen 1988) and the average age of sedimentary mass (Miller *et al*. 1986). Iapetan crust includes normal and depleted island arc tholeiites, and ophiolitic complexes in Newfoundland and Norway (Pedersen & Dunning 1997; MacLachlan & Dunning 1998). Tiñu Formation data are from Murphy *et al*. (2005). CHUR, Chondritic Uniform Reservoir.

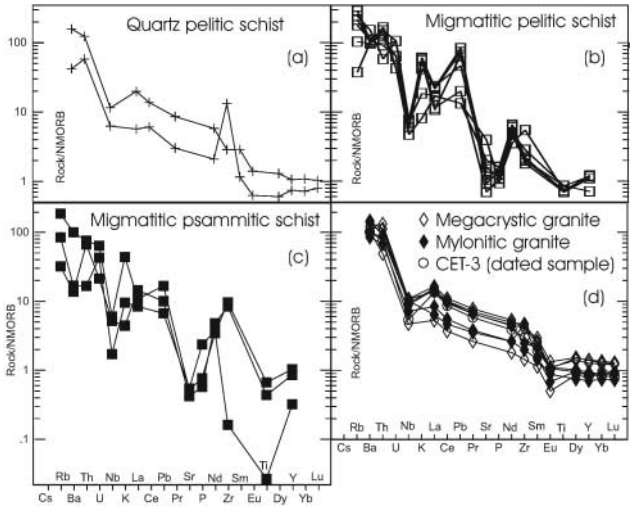

Fig. 13. Spidergrams showing trace element compositions of rocks of the Asís Lithodeme: (**a**) pelitic rocks; (**b**) migmatitic pelitic schist; (**c**) migmatitic psammitic schist; (**d**) granitoid rocks.

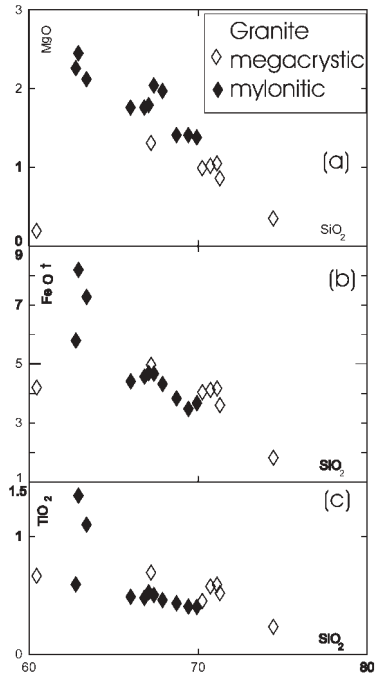

Fig. 14. (**a**) SiO_2 v. MgO, (**b**) SiO_2 v. FeO_t and (**c**) SiO_2 v. TiO_2 for granitoid rocks of the Asís area.

migmatites (Figs 9e and 13c). Some samples display strong enrichment in Zr. However, they have similar $\epsilon_{Nd(t)}$ and T_{DM} values to migmatites with 55–70 wt% SiO_2, although one sample (102-3), has anomalously high $^{147}Sm/^{144}Nd$ (Fig. 12). In general, the trace element, REE and Sm–Nd isotopic characteristics of the migmatites with >55% SiO_2 are similar to those of pelitic and psammitic gneisses.

Granitoid rocks. The megacrystic and mylonitic granitic rocks display very similar geochemical signatures, with SiO_2 ranging from 60.5 and 74.5 wt% and a decrease in FeO_t, TiO_2 and MgO with increasing SiO_2 (Fig. 14). Chondrite-normalized REE patterns show moderate enrichment in LREE ($(La/Sm)_n$ 2.5–5.32), relatively flat HREE with $(La/Yb)_n$ of 1.1–4.1, and exhibit strong negative Eu anomalies (Fig. 9f). MORB-normalized trace element profiles (Fig. 13d) are distinctly enriched in strongly incompatible trace elements, including Th and Ba, are moderately enriched in LREE relative to the HREE and HFSE, and display distinct Nb and Ti negative anomalies. The geochemical characteristics of the dated sample, CET-3, are typical of the megacrystic and mylonitic rocks (e.g. Figs 9f, 12 and 13d). Although these rocks straddle the arc + syncollisional and within-plate boundary on the Nb–Y plot (Fig. 15a), they plot mainly in the arc field on the Rb–(Nb + Y) and Ta–Yb discrimination plots (after Pearce *et al*. 1984; Fig. 15b and c). The Sm–Nd isotopic signature is very different from that of the amphibolites, and is remarkably uniform, with $\epsilon_{Nd(t)}$ ranging from −4.3 to −5.5 ($t = 475$Ma), $^{147}Sm/^{144}Nd$ from 0.12 to 0.14, and T_{DM} from 1.5 to 1.8 Ga. Sample CET-3 lies within this range (Fig. 12). These $\epsilon_{Nd(t)}$ values are considerably lower than those of the amphibolites and are typical of an intra-crustal origin rather than derivation by fractionation of a mafic parent (Fig. 12). A crustal origin is supported by the Nb and Ti anomalies on MORB-normalized plots, the low $^{147}Sm/^{144}Nd$ and high T_{DM}. However, these values are notably higher than those for the pelitic and psammitic gneisses, suggesting that they are not simply derived from partial melting of host rocks, although the possibility of a mixed mafic–metasedimentary source cannot be excluded. Nevertheless, as the granitoid rocks are predominantly crustally derived, the geochemical data alone cannot distinguish between an origin in a coeval arc and inheritance from older crust that was itself formed in an arc environment.

Discussion

Metasedimentary rocks

The pelitic and psammitic gneisses and their migmatized equivalents show remarkable chemical similarities to the unmetamorphosed, Tremadoc Tiñu Formation, which occurs to the east of the Acatlán Complex, where it rests unconformably upon the *c*. 1 Ga Oaxacan Complex (Fig. 1a). The Tiñu Formation contains a Gondwanan fauna (Robison & Pantoja-Alor 1968) and is unconformably overlain by Carboniferous sedimentary rocks containing a Laurentian fauna (Boucot *et al*. 1997). The geochemistry of sandstones and shales of the Tiñu Formation (Murphy *et al*. 2005) also shows a wide range in SiO_2 that, as for the Asís high-grade metasedimentary rocks, is interpreted to reflect derivation from crust with mafic and felsic components. In both cases, the presence of a significant mafic component suggests proximal sources (e.g. Nesbitt & Young 1996). The Tiñu sedimentary rocks display LREE enrichment with a moderate Eu anomaly (Fig. 9c), similarly low $\epsilon_{Nd(t)}$ values (−7.1 to −7.7, calculated for $t = 475$Ma) and Mesoproterozoic T_{DM} ages (1.5–1.83 Ga), and contain detrital zircons that yield ages of 990–1200 Ma (Gillis *et al*. 2001), i.e. similar to those of the Asís psammitic sample, CET-2. The Tiñu Formation data are interpreted to reflect derivation mainly from the underlying Oaxacan Complex with little or no input from distal or juvenile sources. Minor input from the Amazon craton may be indicated by the *c*. 1300–1660 Ma detrital zircons, and the youngest *c*. 700 Ma detrital zircon could have come from either Amazonia or Avalonia (Fig. 16). The similarities in geochemistry, Sm–Nd isotopes and ages of detrital zircons between the high-grade metasedimentary rocks of the Asís Lithodeme and the Tiñu Formation suggests that protoliths of the Asís metasedimentary

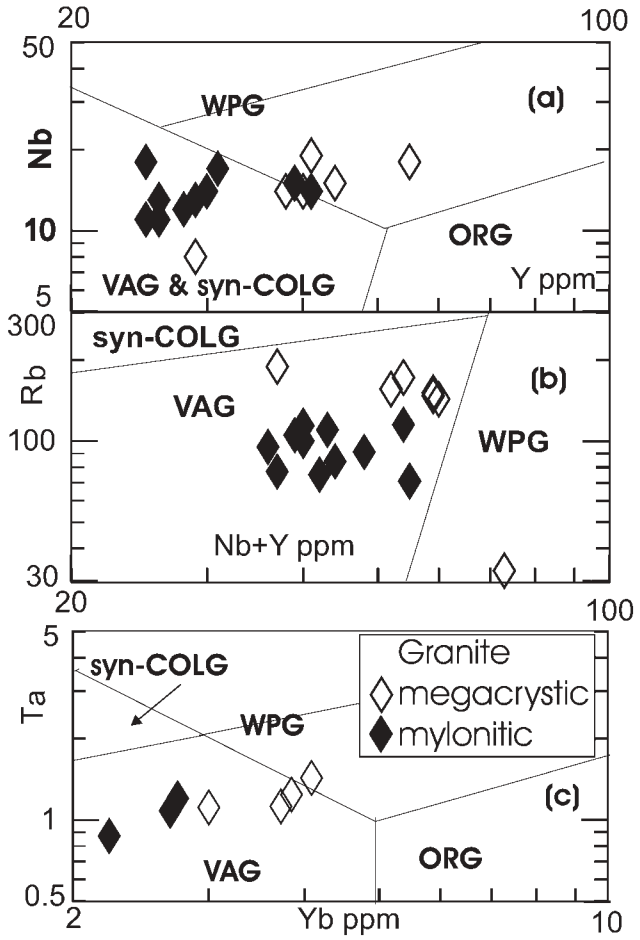

Fig. 15. (**a**) Nb v. Y, (**b**) Rb v. Nb + Y and (**c**) Ta v. Yb discrimination plots for granitoid rocks of the Asís Lithodeme (after Pearce *et al*. 1984). WPG, within-plate granite; VAG, volcanic arc granite; syn-COLG, syncollisional granite; ORG, ocean ridge granite.

rocks are also derived from the Oaxacan Complex (Keppie *et al*. 2001, 2003*a*; Cameron *et al*. 2004; Ortega-Obregón *et al*. 2003; Solari *et al*. 2004). This is consistent with their high T_{DM} ages, which suggest derivation from Mesoproterozoic crust. Their variable major and trace element chemistry from intermediate to highly siliceous composition suggests that they represent rift-related and/or passive margin sedimentary rocks. Although poorly constrained, the *c*. 700–470 Ma age bracket for deposition of the Asís Lithodeme, together with indistinguishable geochemical, isotopic and detrital zircon population characteristics, is consistent with correlation of the protoliths with the Tremadoc Tiñu Formation, and therefore, as for the Tiñu Formation, an origin along the Gondwanan margin of the Rheic Ocean.

Amphibolites

The amphibolites and migmatitic amphibolites have geochemical signatures typical of differentiated continental tholeiites, with relatively little evidence for crustal contamination suggesting a thinned crust and/or an extensional setting. Elías-Herrera *et al*. (2004) reported ages of 442 ± 2 Ma for a zircon core with rims dated at *c*. 360–345 Ma (U–Pb SHRIMP ages) that are here interpreted as protolith and eclogite-facies metamorphism, respectively. The latter age is similar to *c*. 346 Ma age of metamorphism reported by Middleton *et al*. (2005), and the *c*. 442 Ma age falls within the range of ages determined for the quartz-augen granite (this paper) and other megacrystic granitoids in the Acatlán Complex (Sánchez-Zavala *et al*. 2004; Miller *et al*. 2005). This suggests that the amphibolites and the granitoids in the Asís Lithodeme are coeval and represent a bimodal suite.

The T_{DM} ages of the amphibolites range from 0.75 to 1.27 Ga, indicative of derivation from continental mantle lithosphere. Such T_{DM} ages are common in igneous complexes along the northern Gondwanan margin, and are interpreted to reflect ancestral crust and mantle lithospheric components that formed in the peri-Rodinian ocean between 1.2 and 0.75 Ga, were accreted to the Amazonian margin of Gondwana in the late

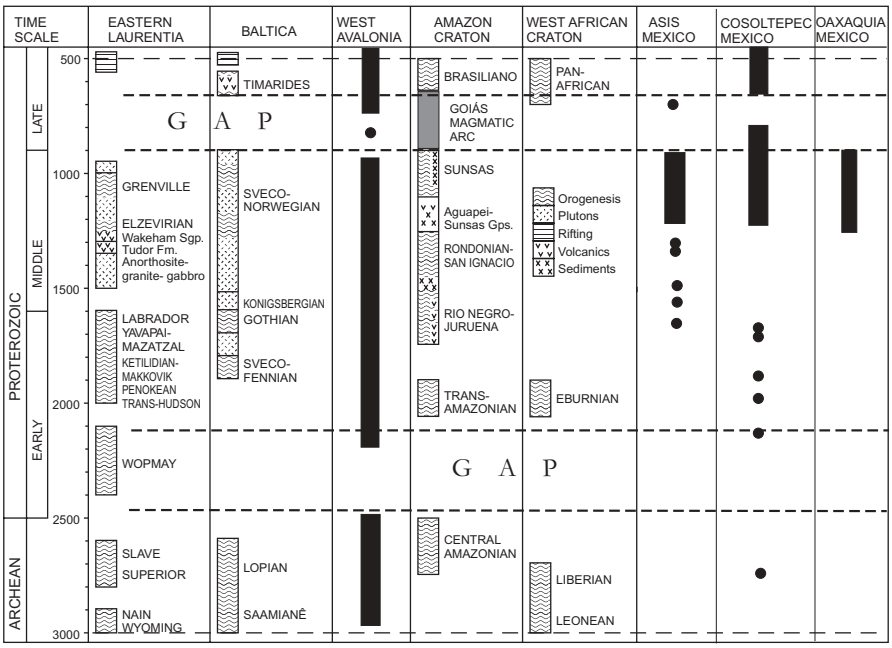

Fig. 16. Comparison of detrital zircon ages from the Asís Lithodeme with the Cosoltepec Formation (Keppie *et al*. 2006), and potential source regions (modified after Murphy *et al*. 1999).

Neoproterozoic and subsequently recycled during Palaeozoic tectonic events (Murphy *et al*. 2000, 2004). This situation may be analogous to Mesozoic–Cenozoic terrane accretion in the Canadian Cordillera, where recent studies have shown that such accretion can be thick skinned, incorporating the mantle lithosphere to a depth of *c*. 150 km (McKenzie *et al*. 2005).

Granitoid rocks

Field relationships (Middleton *et al*. 2005) and similar geochemical and isotopic characteristics suggest that the mylonitic granite is the deformed equivalent of the *c*. 470–420 Ma megacrystic granitoids. Their 1.5–1.8 Ga, T_{DM} ages are very similar to those of the *c*. 1 Ga basement of Oaxaquia, which are: (1) 1.4–1.6 Ga for meta-igneous rocks; (2) 1.5–2.0 Ga for the metasedimentary rocks (Patchett & Ruiz 1987; Ruiz *et al*. 1988; Weber & Köhler 1999). These characteristics suggest that the granitic magma was derived by crustal anatexis from a basement similar to Oaxaquia, which is inferred to underlie the Acatlán Complex (Keppie 2004). Their geochemistry is very similar to that of Ordovician undeformed granitoid plutons in the northern Acatlán Complex (Miller *et al*. 2005). Although these geochronological data do not sufficiently resolve the relative timing of basaltic and granitoid magmatism in the Asís Lithodeme, regional considerations are consistent with the interpretation that the amphibolites and the granitoids in the Asís Lithodeme may represent a bimodal suite.

Summary and conclusions

According to Talavera-Mendoza *et al*. (2005), the Acatlan Complex reflects *c*. 480–470 Ma SE-vergent subduction, and high-pressure (eclogite- and blueschist-facies metamorphism) during which time the Piaxtla Suite accreted to Laurentia. If correct, the Acatlan Complex would have originated within the Iapetus Ocean. However, a concordant U–Pb zircon (isotope dilution thermal ionization mass spectrometry) age of 346 ± 3 Ma from a Piaxtla Suite eclogite and *c*. 345 Ma SHRIMP analysis from a Piaxtla Suite migmatite (Middleton *et al*. 2005) indicate that the Asís Lithodeme underwent eclogite-facies metamorphism followed by rapid exhumation in the Carboniferous (Middleton *et al*. 2005), implying that the Asís protoliths could not have formed within the Iapetus Ocean, which closed in the Silurian.

The lithologies of the Asís area could have formed along the Gondwanan flank of the Rheic Ocean during the rifting of Avalonia from Gondwana. The combination of within-plate continental tholeiitic mafic rocks, crustally derived granitoids, and continentally derived clastic rocks suggests that the Asís Lithodeme protoliths represent a rift–passive margin sequence. Although the age constraints on the time of deposition of the metasedimentary rocks are rather wide (*c*. 700–420 Ma), the Tremadoc age of the adjacent Tiñu Formation provides a minimum age for initiation of the passive margin sequence. As Oaxaquia remained along the Gondwanan margin until Carboniferous collision with Laurussia, the data suggest that some terrane rifted from the Oaxacan portion of the Gondwanan margin in the Tremadoc. Most recent palinspastic reconstructions place Avalonia adjacent to Oaxaquia and Amazonia in the late Neoproterozoic (e.g. Keppie *et al*. 2003*b*, and references therein). Although Prigmore *et al*. (1997) inferred that Avalonia separated from Gondwana in the Late Cambrian to early Tremadoc based upon subsidence curves, they documented three episodes of rapid subsidence in Avalonia: Early Cambrian, Late Cambrian–Tremadoc, and Late Ordovician. Landing (1996, 2004) has suggested that the distinct Avalonian fauna indicates rifting and separation of Avalonia from Gondwana in the latest Neoproterozoic to Early Cambrian, which is consistent with the Early Cambrian rapid subsidence recorded in Avalonia (Prigmore *et al*. 1997). However, Avalonian fauna gradually become indistinguishable from Gondwanan fauna in the Late Cambrian and Early Ordovician (Fortey & Cocks 2003; Landing 2005), suggesting that Early Cambrian rifting resulted in the development of a narrow seaway and that Avalonia essentially retained its peri-Gondwanan location. Keppie *et al*. (2003*b*) proposed that late Neoproterozoic collision of an ocean ridge with the subducting northern margin of Gondwana produced a Baja California type of margin, resulting in transtensional rifting and separation of Avalonia in the Cambrian. It is inferred that Avalonia moved along the Gondwanan margin with the fauna gradually managing to cross the small ocean barrier.

Faunal and palaeomagnetic data (e.g. Cocks & Torsvik 2002; Fortey & Cocks 2003) indicate that Avalonia drifted about 1800 km north of the Gondwanan margin between 485 and 460 Ma (Hamilton & Murphy 2004), ending its peri-Gondwanan affinity (Fig. 17). This drift of Avalonia from the Gondwanan margin resulted in the formation of the Rheic Ocean, and corresponds to the second phase of subsidence documented by Prigmore *et al*. (1997).

The data presented herein, however, cannot distinguish between the various mechanisms proposed for the origin of the Rheic Ocean. According to Van Staal *et al*. (1998), the Rheic

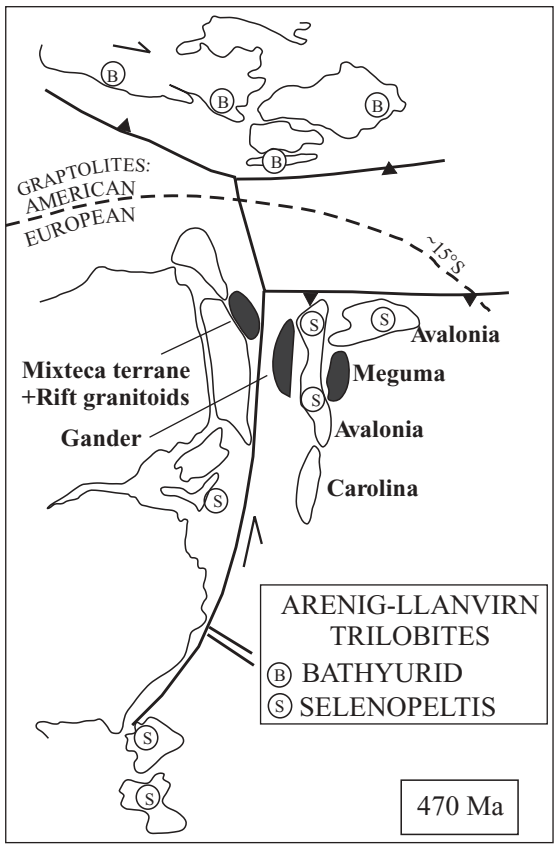

Fig. 17. Palaeogeographical reconstruction for *c*. 470 Ma showing the location of the Asís Lithodeme in the Acatlán complex of the Mixteca terrane on the southern margin of the Rheic Ocean (modified after Keppie 2004).

Ocean started as a back-arc basin, but evidence for arc-related rocks coeval with rifting along the Gondwanan margin is equivocal. In this case, the protoliths of the Asís Lithodeme may have formed on a continental margin inboard of a rifted arc.

As the opening of the Rheic Ocean is coeval with the onset of NW-directed subduction and ridge–trench collision along the Laurentian margin (see Van Staal *et al*. 1998; Stampfli & Borel 2002), the origin of the Rheic Ocean may be geodynamically linked to slab pull (Murphy *et al*. 2006) in a manner analogous to the opening of Neotethys in the Cenozoic (Stampfli & Borel 2002). In this scenario the protoliths of the Asís Lithodeme may have formed in a continental rift environment.

We would like to acknowledge NSERC Discovery grants to J.B.M. and J.D., Papiit grant IN103003 to J.D.K., and NSF grants (EAR 0308105 and EAR-0456180) to R.D.N. and B.V.M., and an Ohio University 1804 Award to R.D.N. and J. Wooden at Stanford SHRIMP facility. We would also like to thank M. Morales for assistance with drawing the figures, and J. Hibbard and C. Quesada for their constructive comments. This paper is a contribution to IGCP Project 497 (The Rheic Ocean).

References

Ayer, J.A. & Davis, D.W. 1997. Neoarchean evolution of differing convergent margin assemblages in the Wabigoon Subprovince: geochemical and geochronological evidence from the Lake of the Woods greenstone belt, Superior Province, northwestern Ontario. *Precambrian Research*, **81**, 155–178.

Boucot, A.J., Blodgett, R.B. & Stewart, J.H. 1997. European Province Late Silurian bachiopods from the Ciudad Victoria area, Tamaulipas, northeastern Mexico. *In:* Klapper, G., Murphy, M.A. & Talent, J.A. (eds) *Paloeozoic Sequence Stratigraphy, Biostratigraphy, and Biogeography: Studies in Honour of J. Granville ('Jess') Johnson*. Geological Society of America, Special Papers, **321**, 273–293.

Cameron, K.L., Lopez, R., Ortega-Gutiérrez, F., Solari, L.A., Keppie, J.D. & Schulze, C. 2004. U–Pb constraints and Pb isotopic compositions of leached feldspars: constraints on the origin and evolution of Grenvillian rocks from eastern and southern Mexico. *In:* Tollo, R.P., Corriveau, L., McLelland, J. & Bartholomew, M.J. (eds) *Proterozoic Tectonic Evolution of the Grenville Orogen in North America*. Geological Society of America, Memoirs, **197**, 755–770.

Carswell, D.A. 1990. Eclogites and the eclogite facies: definitions and classifications. *In:* Carswell, D.A. (ed.) *Eclogite Facies Rocks*. Blackie, Glasgow, 1–13.

Cocks, L.R.M. & Torsvik, T.H. 2002. Earth geography from 500 to 400 million years ago: A faunal and palaeomagnetic review. *Journal of the Geological Society, London*, **159**, 631–644.

Daly, J.S. & McLelland, J.M. 1991. Juvenile Middle Proterozoic crust in the Adirondack Highlands, Grenville Province, northeastern North America. *Geology*, **19**, 119–122.

Degraaff-Surpless, K., Graham, S.A., Wooden, J.L. & McWilliams, M.O. 2002. Detrital zircon provenance analysis of the Great Valley Group,-California: evolution of an arc–forearc system. *Geological Society of America Bulletin*, **114**, 1564–1580.

Derycke-Khatir, C., Vachard, D., Dégardin, J.-M., Flores de Dios, A., Buitrón, B. & Hansen, M. 2005. Late Pennsylvanian and Early Permian chondichthyan microremains from San Salvador Patlanoaya (Puebla, Mexico). *Geobios*, **38**, 43–55.

Dickin, A.P. 2000. Crustal formation in the Grenville Province: Nd isotopic evidence. *Canadian Journal of Earth Sciences*, **37**, 165–181.

Dickin, A.P. & McNutt, R.H. 1989. Nd model age mapping of the southeast margin of the Archean foreland in the Grenville Province of Ontario. *Geology*, **17**, 299–302.

Dickin, A.P. & McNutt, R.H. 1990. Nd model-age mapping of Grenville lithotectonic domains: Mid-Proterozoic crustal evolution in Ontario. *In:* Gower, G.F., Rivers, T. & Ryan, B. (eds) *Mid-Proterozoic Laurentia–Baltica*. Geological Association of Canada, Special Papers, **38**, 79–94.

Dostal, J., Baragar, W.R.A. & Dupuy, C. 1986. Petrogenesis of the Natkusiak continental basalts, Victoria Island, N.W.TÒ *Canadian Journal of Earth Sciences*, **23**, 622–632.

Dostal, J., Keppie, J.D., Nance, R.D., Miller, B.V. & Cooper, P. 2004. Xayacatlán Formation, Acatlán Complex, southern Mexico: tectonic implications. *In: IV Reunion Nacional de Ciencias de la Tierra, Libro de Resumenes*. 151.

Elías-Herrera, M. & Ortega-Gutiérrez, F. 2002. Caltepec fault zone: an Early Permian dextral transpressional boundary between the Proterozoic Oaxacan and Paleozoic Acatlán complexes, southern Mexico, and regional implications. Tectonics, **21**(3), 101029/200TC001278.

Elías-Herrera, M., Ortega-Gutiérrez, F., Sánchez-Zavala, J.L., Reyes-Salas, A.M., Macias-Romo, C. & Iriondo, A. 2004. New geochronological and stratigraphic data related to the Paleozoic evolution of the high-pressure Piaxtla Group, Acatlán Complex, southern Mexico. *In:* Editor, A. (ed.) *IV Reunion Nacional de Ciencias de la Tierra, Libro de Resumenes*. 150.

Fernández-Suárez, J., Gutiérrez-Alonso, G. & Jeffries, T.E. 2002. The importance of along-margin terrane transport in northern Gondwana: insights from detrital zircon parentage in Neoproterozoic rocks from Iberia and Brittany. *Earth and Planetary Science Letters*, **204**, 75–88.

Fortey, R. A. & Cocks, L.R.M. 2003. Palaeontological evidence bearing on global Ordovician-Silurian continental reconstructions. *Earth Science Reviews*, **61**, 245–307.

Gillis, R.J., Gehrels, G.E., Flores de Dios, A. & Ruiz, J. 2001. Paleogeographic implications of detrital zircon ages from the Oaxaca terrane of southern Mexico. *Geological Society of America, Abstracts with Programs*, **88**, A-428.

Goldstein, S.J. & Jacobsen, S.B. 1988. Nd and Sr isotopic systematics of river water suspended material: implications for crustal evolution. *Earth and Planetary Science Letters*, **87**, 249–265.

Hamilton, M.A. & Murphy, J.B. 2004. Tectonic significance of a Llanvirn age for the Dunn Point volcanic rocks, Avalon terrane, Nova Scotia, Canada: implications for the evolution of the Iapetus and Rheic oceans. *Tectonophysics*, **379**, 199–209.

Jeffries, T., Fernández-Suárez, J., Corfu, F. & Gutiérrez Alonso, G. 2003. Advances in U–Pb geochronology using a frequency quintupled Nd:YAG based laser ablation system ($\lambda = 213$nm) and quadrupole based ICP-MS. *Journal of Analytical Atomic Spectrometry*, **18**, 847–855.

Keppie, J.D. 2004. Terranes of Mexico revisited: a 1.3 billion year odyssey. *International Geology Review*, **46**, 765–794.

Keppie, J.D. & Ramos, V.S. 1999. Odyssey of terranes in the Iapetus and Rheic Oceans during the Paleozoic. *In:* Ramos, V.S. & Keppie, J.D. (eds) *Laurentia–Gondwana Connections before Pangea*. Geological Society of America, Special Papers, **336**, 267–276.

Keppie, J.D., Dostal, J., Ortega-Gutierrez, F. & Lopez, R. 2001. A Grenvillian arc on the margin of Amazonia: evidence from the southern Oaxacan Complex, southern Mexico. *Precambrian Research*, **112**, 165–181.

Keppie, J.D., Dostal, J., Cameron, K.L., Solari, L.A., Ortega-Gutiérrez, F. & Lopez, R. 2003a. Geochronology and geochemistry of Grenvillian igneous suites in the northern Oaxacan Complex, southern México: tectonic implications. *Precambrian Research*, **120**, 365–389.

Keppie, J.D., Nance, R.D., Murphy, J.B. & Dostal, J. 2003b. Tethyan, Mediterranean, and Pacific analogues for the Neoproterozoic–Paleozoic birth and development of peri-Gondwanan terranes and their transfer to Laurentia and Laurussia. *Tectonophysics*, **365**, 195–219.

Keppie, J.D., Sandberg, C.A., Miller, B.V., Sánchez-Zavala, J.L., Nance, R.D. & Poole, F.G. 2004a. Implications of latest Pennsylvanian to Middle Permian paleontological and U–Pb SHRIMP data from the Tecomate Formation to re-dating tectonothermal events in the Acatlán Complex, southern Mexico. *International Geology Review*, **46**, 745–754.

Keppie, J.D., Nance, R.D. & Powell, J.T. *et al.* 2004b. Mid-Jurassic tectonothermal event superposed on a Paleozoic geological record in the Acatlán Complex of southern Mexico: hotspot activity during the breakup of Pangea. *Gondwana Research*, **7**, 239–260.

Keppie, J.D., Nance, R.D., Fernández-Suárez, J., Storey, C.D., Jeffries, T.E. & Murphy, J.B. 2006. Detrital zircon data from the eastern Mixteca terrane, southern Mexico: evidence for an Ordovician–Mississippian continental rise and a Permo-Triassic clastic wedge adjacent to Oaxaquia. *International Geology Review*, **48**, 97–111.

Kerr, A., Jenner, G.A. & Fryer, B.J. 1995. Sm–Nd isotopic geochemistry of Precambrian to Paleozoic granitoid suites and the deep-crustal structure of the southeast margin of the Newfoundland Appalachians. *Canadian Journal of Earth Sciences*, **32**, 224–245.

Landing, E. 1996. Avalon: insular continent by the latest Precambrian. *In:* Nance, R.D. & Thompson, M.D. (eds) *Avalonian and Related Peri-Gondwanan Terranes of the Circum-North Atlantic*. Geological Society of America, Special Papers, **304**, 29–63.

Landing, E. 2004. Precambrian–Cambrian boundary interval deposition and the marginal platform of the Avalon microcontinent. *Journal of Geodynamics*, **37**, 411–435.

Landing, E. 2005. Early Paleozoic Avalon-Gondwana unity: An obituary-response to "Palaeontological evidence bearing on global Ordovician-Silurian continental reconstructions" by R.A. Fortey and L.R.M. Cocks: Discussion. *Earth Science Reviews*, **69**, 169–175.

Ludwig, K.R. 1989. *Pb-Dat: a computer program for processing raw Pb-U-Th isotope data*. USGS Open-File Report. **88-557**.

Mackenzie, J.M., Canil, D., Johnston, S.T., English, J., Mihalynuk, M.G. &

Grant, B. 2005. First evidence for ultrahigh-pressure garnet peridotite in the North American Cordillera. *Geology*, **33**, 105–108.

MacLachlan, K. & Dunning, G.R. 1998. U–Pb ages and tectonomagmatic relationships of early Ordovician low-Ti tholeiites, boninites, and related plutonic rocks in central Newfoundland. *Contributions to Mineralogy and Petrology*, **133**, 235–258.

Malone, J.W., Nance, R.D., Keppie, J.D. & Dostal, J. 2002. Deformational history of part of the Acatlán Complex: Late Ordovician–Early Silurian and Early Permian orogenesis in southern Mexico. *Journal of South American Earth Sciences*, **15**, 511–524.

McLelland, J.M., Daly, J.S. & Chiarenzelli, J. 1993. Sm–Nd and U–Pb isotopic evidence of juvenile crust in the Adirondack lowlands and implications for the evolution of the Adirondack Mts. *Journal of Geology*, **101**, 97–105.

Meza-Figueroa, D., Ruiz, J., Talavera-Mendoza, O. & Ortega-Gutiérrez, F. 2003. Tectonometamorphic evolution of the Acatlan Complex eclogites (southern Mexico). *Canadian Journal of Earth Sciences*, **40**, 27–44.

Middleton, M.D., Keppie, J.D., Murphy, J.B., Miller, B.V. & Nance, R.D. 2006. *P–T–t* constraints on exhumation following subduction in the Rheic Ocean: eclogitic Asís Lithodeme, Piaxtla Suite, Acatlán Complex, southern Mexico. *In:* Linnemann, U., Nance, R.D., Zulauf, G. & Kraft, P. (eds) *The Geology of Peri-Gondwana: The Avalonian-Cadomian Belt, Adjoining Cratons and the Rheic Ocean*. Geological Society of America, Special Papers, in press.

Miller, B.V., Dostal, J., Keppie, J.D., Nance, R.D., Ortega-Rivera, A. & Lee, J.K.W. 2006. Ordovician calc-alkaline granitoids in the Acatlán Complex, southern Mexico: geochemical and geochronological evidence for either rifting or subduction along the Gondwanan margin of the Rheic Ocean. *In:* Linnemann, U., Nance, R.D., Zulauf, G. & Kraft, P. (eds) *The Geology of Peri-Gondwana: The Avalonian-Cadomian Belt, Adjoining Cratons and the Rheic Ocean*. Geological Society of America, Special Papers, in press.

Miller, R.G., O'Nions, R.K., Hamilton, P.J. & Welin, E. 1986. Crustal residence ages of clastic sediments, orogeny, and crustal evolution. *Chemical Geology*, **57**, 87–99.

Miyashiro, A. 1974. Volcanic rock series in island arcs and active continental margins. *American Journal of Science*, **274**, 321–355.

Murphy, J.B. & Macdonald, D.A. 1993. Geochemistry of late Proterozoic arc-related volcaniclastic turbidite sequences, Antigonish Highlands, Nova Scotia. *Canadian Journal of Earth Sciences*, **30**, 2273–2282.

Murphy, J.B., Keppie, J.D., Dostal, J. & Cousens, B.L. 1996. Repeated lower crustal melting beneath the Antigonish Highlands, Avalon Composite Terrane, Nova Scotia: Nd isotopic evidence and tectonic implications. *In:* Nance, R.D. & Thompson, M.D. (eds) *Avalonian and Related Peri-Gondwanan Terranes of the Circum North Atlantic*. Geological Society of America, Special Papers, **304**, 109–120.

Murphy, J.B., Keppie, J.D., Dostal, J. & Nance, R.D. 1999. Neoproterozoic-Early Paleozoic evolution of Avalonia and Cenozoic analogues. *In:* Ramos, V. & Keppie, J.D. (eds) *Laurentia-Gondwana connections before Pangea*. Geological Society of America Special Papers, **336**, 253–266.

Murphy, J.B., Strachan, R.A., Nance, R.D., Parker, K.D. & Fowler, M.B. 2000. Proto-Avalonia: a 1.2–1.0 Ga tectonothermal event and constraints for the evolution of Rodinia. *Geology*, **28**, 1071–1074.

Murphy, J.B., Fernandez-Suarez, J. & Jeffries, T.E. 2004. Lithogeochemical, Sm–Nd and U–Pb isotopic data from the Silurian–Early Devonian Arisaig Group clastic rocks, Avalon terrane, Nova Scotia: a record of terrane accretion in the Appalachian–Caledonide orogen. *Geological Society of America Bulletin*, **116**, 1183–1201.

Murphy, J.B., Keppie, J.D., Braid, J.F. & Nance, R.D. 2005. Geochemistry of the Tremadocian Tiñu Formation (Southern Mexico): provenance in the underlying *c*. 1 Ga Oaxacan Complex on the southern margin of the Rheic Ocean. *International Geology Review*, **47**, 887–900.

Murphy, J.B., Gutierrez-Alonso, G., Nance, R.D., Fernandez-Suarez, J., Keppie, J.D., Quesada, C., Strachan, R.A. & Dostal, J. 2006. Origin of the Rheic Ocean: rifting along a Neoproterozoic suture? *Geology*, **34**, 325–328.

Nesbitt, H.W. & Young, G.M. 1996. Petrogenesis of sediments in the absence of chemical weathering: effects of abrasion and sorting on bulk composition and mineralogy. *Sedimentology*, **43**, 341–358.

Ortega-Gutiérrez, F., Elías-Herrera, M., Reyes-Salas, M., Macias-Romo, C. & López, R. 1999. Late Ordovician–Early Silurian continental collision orogeny in southern Mexico and its bearing on Gondwana–Laurentia connections. *Geology*, **27**, 719–722.

Ortega-Obregón, C., Keppie, J.D. & Solari, L.A. *et al*. 2003. Geochronology and geochemistry of the *c*. 917 Ma, calc-alkaline Etla granitoid pluton (Oaxaca, southern Mexico): evidence of post-Grenvillian subduction along the northern margin of Amazonia. *International Geology Review*, **45**, 596–610.

Patchett, P.J. & Ruiz, J. 1987. Nd isotopic ages of crustal formation and metamorphism in the Precambrian of eastern and southern Mexico. *Contributions to Mineralogy and Petrology*, **96**, 523–528.

Pearce, J.A. & Norry, M.J. 1979. Petrogenetic implications of Ti, Zr, Y, and Nb variations in volcanic rocks. *Contributions to Mineralogy and Petrology*, **69**, 33–47.

Pearce, J.A., Harris, N.B.W. & Tindle, A.G. 1984. Trace element discrimination diagrams for the tectonic interpretation of granitic rocks. *Journal of Petrology*, **25**, 956–983.

Pedersen, R.B. & Dunning, G.R. 1997. Evolution of arc crust and relations between contrasting sources: U–Pb (age), Nd, Sr isotopic systematics of the ophiolite terrain of SW Norway. *Contributions to Mineralogy and Petrology*, **128**, 1–15.

Prigmore, J.K., Butler, A.J. & Woodcock, N.H. 1997. Rifting during separation of Eastern Avalonia from Gondwana: evidence from subsidence analysis. *Geology*, **25**, 203–206.

Robison, R. & Pantoja-Alor, J. 1968. Tremadocian trilobites from Nochixtlan region, Oaxaca, Mexico. *Journal of Paleontology*, **42**, 767–800.

Ruiz, J., Patchett, P.J. & Ortega-Gutiérrez, F. 1988. Proterozoic and Phanerozoic basement terranes of Mexico from Nd isotopic studies. *Geological Society of America Bulletin*, **100**, 274–281.

Ruiz, J., Talavera-Mendoza, O. & Gehrels, G. 2004. Correlation of Paleozoic and Proterozoic terranes of southern Mexico with the northern Andes based on U–Pb geochronology of detrital zircons. *In: IV Reunion Nacional de Ciencias de la Tierra, Libro de Resumenes*. 198.

Sánchez Zavala, J.L., Ortega Gutiérrez, F. & Elías Herrera, M. 2000. La orogenia Mixteca del Devonico del Complejo Acatlán, sur de Mexico. *In: GEOS, Union Geophysica Mexicana, 2nd Reunion Nacional de Ciencias de la Tierra, Resumenes y Programa*. **20(3)**, 321–322.

Sánchez-Zavala, J.L., Ortega-Gutiérrez, F., Keppie, J.D., Jenner, G.A. & Belousova, E. 2004. Ordovician and Mesoproterozoic zircon from the Tecomate Formation and Esperanza granitoid, Acatlán Complex, southern Mexico: local provenance in the Acatlán and Oaxacan complexes. *International Geology Review*, **46**, 1005–1021.

Solari, L.A., Keppie, J.D., Ortega-Gutiérrez, F., Cameron, K.L., Lopez, R. & Hames, W.E. 2004. 990 Ma and 1,100 Ma Grenvillian tectonothermal events in the northern Oaxacan Complex, southern Mexico: roots of an orogen. *Tectonophysics*, **365**, 257–282.

Stampfli, G.M. & Borel, G.D. 2002. A plate tectonic model for the Paleozoic and Mesozoic constrained by dynamic plate boundaries and restored synthetic oceanic isochrones. *Earth and Planetary Science Letters*, **196**, 17–33.

Sun, S.S. & McDonough, W.F. 1989. Chemical and isotopic systematics of oceanic basalts: implications for mantle composition and processes. *In:* Saunders, A.D. & Norry, M.J. (eds) *Magmatism in the Ocean Basins*. Geological Society, London, Special Publications, **42**, 313–345.

Talavera-Mendoza, O., Ruíz, J., Gehrels, G.E., Meza-Figueroa, D.M., Vega-Granillo, R. & Campa-Uranga, M.F. 2005. U–Pb geochronology of the Acatlán Complex and implications for the Paleozoic paleogeography and tectonic evolution of southern Mexico. *Earth and Planetary Science Letters*, **235**, 682–699.

Vachard, D. & Flores de Dios, A. 2002. Discovery of latest Devonian/earliest Mississippian microfossils in San Salvador Patlanoaya (Puebla, Mexico); biogeographic and geodynamic consequences. *Comptes Rendus de l'Académie des Sciences, Geoscience*, **334**, 1095–1101.

Van Staal, C.R., Dewey, J.F., Mac Niocaill, C. & McKerrow, W.S. 1998. The Cambrian–Silurian tectonic evolution of the Northern Appalachians and British Caledonides: history of a complex, west and southwest Pacific-type segment of Iapetus. *In:* Blundell, D. & Scott, A.C. (eds) *Lyell: The Past is the Key to the Present*. Geological Society, London, Special Publications, **143**, 199–242.

Weber, B. & Köhler, H. 1999. Sm/Nd, Rb/Sr, and U–Pb geochronology of a Grenville terrane in southern Mexico: origin and geologic history of the Guichicovi complex. *Precambrian Research*, **96**, 245–262.

Received 18 July 2005; revised typescript accepted 1 November 2005.
Scientific editing by Martin Whitehouse